Mercier R, Kawai Y, Errington J.

Wall proficient *E-coli* capable of sustained growth in the absence of the Z-ring division machine.

***Nature Microbiology* 2016, 1(8), 16091.**

Wall proficient *E. coli* capable of sustained growth in the absence of the Z-ring division machine

Romain Mercier[1,2,*], Yoshikazu Kawai[1] and Jeff Errington[1,*]

[1]Centre for Bacterial Cell Biology, Institute for Cell and Molecular Biosciences, Medical School, Newcastle University, Richardson Road, Newcastle upon Tyne NE2 4AX, UK

[2]Laboratoire de Chimie Bactérienne, Institut de Microbiologie de la Méditerranée, CNRS-Aix-Marseille University, 31 Chemin Joseph Aiguier, 13009 Marseille, France

*Correspondence: rmercier@imm.cnrs.fr and jeff.errington@ncl.ac.uk

Summary

The peptidoglycan (PG) cell wall is a major protective external sheath in bacteria and a key target for antibiotics[1]. PG is present in virtually all bacteria, suggesting that it has a very ancient origin, and was likely present in the last bacterial common ancestor[2]. Cell wall expansion is orchestrated by cytoskeletal proteins related to actin (MreB) and tubulin (FtsZ)[3], which also emerged very early in evolution. FtsZ has been characterised in a wide range of organisms and is a key essential player in a highly organised division machine that directs an invaginating annulus of cell wall PG, together with the other various cell envelope layers. MreB plays an analogous role in directing growth of the lateral wall in cylindrical (rod shaped) organisms, which comprise the majority of extant bacterial forms. Recent work on cell wall-less derived bacteria, called L-forms, has revealed that these cells require neither MreB nor FtsZ for growth and division[4-6], consistent with the notion that these proteins are concerned exclusively with wall dynamics. Discovery that *ftsZ* can be deleted in an L-form background recently provided, for the first time, a means of generating an *ftsZ* null mutant of *E. coli*. Remarkably, starting with this strain we have been able to isolate variants of *E. coli* that lack FtsZ but are capable of efficient growth in a walled state. Genetic analysis reveals that a combination of three mutations is needed for this phenotype. Importantly, the suppressive mutations lead to a major cell shape change, from the normal cylindrical shape to a branched and bulging, ramified shape, which we call “coli-flower”. The results highlight the versatility and adaptability of bacterial cells and illustrate possible evolutionary routes leading to the emergence of specialised bacteria such as pathogenic Chlamydia or aquatic Planctomycetes, that lack FtsZ but retain the PG cell wall[7-9].

Results and discussions

Cell wall-free bacteria, also called L-forms, can regenerate their parental cell morphology in the absence of a pre-existing template[6,10]. In *E. coli*, the recovery of a walled rod-shaped morphology from a pleiomorphic L-form requires only a few cell division events[11,12]. Here, we investigated the requirement of cell division events in the recovery process using an *E. coli* L-form strain lacking the essential cell division *ftsZ* gene (Fig. 1a). As previously observed, when wild-type *E. coli* L-forms were cultured in the absence of a cell wall inhibitor, but presence of an osmotic stabiliser, the cells readily resumed growth and reverted to the rod-shaped walled state (Fig. 1b, top panels)[6,11,12]. In contrast, L-forms of the *ftsZ* deleted strain failed to grow under these conditions (Fig. 1b, bottom left panel). Microscopic observation revealed the presence of non-dividing filamentous cells in the *ftsZ*-deleted strain (Fig. 1b, bottom right panel), showing that the cells are capable of resuming normal rod-shaped growth in the absence of a functional division apparatus, even though they cannot sustain long term proliferation.

Unexpectedly, after prolonged incubation of a plate bearing an *ftsZ*-deleted strain, several colonies appeared, presumably containing cell variants capable of growth (Supplementary Fig. 1a). After confirming that the colonies were variants of the original strain rather than contaminants, we tested their properties and found that they were of two general classes. One class had resumed growth as L-forms, presumably by acquiring mutations that block cell wall synthesis, and these were not studied further. The second class of mutants (CFL; coli-flower), however, appeared to comprise walled cells, and several lines of evidence suggested that these were mutants capable of walled growth in the absence of FtsZ. First, unlike L-forms, the CFL mutants were able to grow in either the absence or the presence of osmotic stabilisers (Supplementary Fig. 1b and 1c, right and left panels), although magnesium was needed to stabilise the CFL cells (Supplementary Fig. 1b-c, middle and right panels, and 1e-f, Supplementary video 1). Second, the CFL mutants grew in liquid media (Supplementary Fig. 1d), while *E. coli* L-forms are unable to proliferate under these

conditions[6]. Finally, in contrast to L-forms, the CFL mutant strains were highly sensitive to *β*-lactam antibiotics (Fig. 1c, Supplementary Fig. 1g).

In previous reports of experiments with FtsZ impaired strains, the cells were shown to continue to elongate normally for a few generation times, forming filamentous cells with approximately normal diameter (Fig. 1b, bottom right panel) but eventually all of the filaments lysed, with no long-term survivors (e.g.[13]). However, the CFL mutant cells turned out not to be filamentous but instead had a bulging, branching and highly pleiotropic morphology, which we call “coli-flower” (Fig. 1d). Typically, the cells tend to have several peripheral spherical areas, of differing size, connected to a central branched zone, which sometimes has a more or less cylindrical shape but with varying width. Interestingly, despite the pleiotropy of cell morphology, DNA staining revealed a relatively homogeneous distribution of chromosomal DNA in the cell, both in the branching and spherical areas (Supplementary Fig. 2). Remarkably, when we reintroduced the *ftsZ* gene into a CFL mutant strain an almost normal rod shaped cell morphology was returned (Fig. 1e, Supplementary Fig. 3a-d), revealing that none of the putative *ftsZ*-suppressing mutations are required to maintain the wild type cell shape. Batch cultures of the CFL mutants showed a biphasic growth pattern, with a mass doubling time of about 60 min in exponential phase (Fig. 1f and Supplementary Fig. 4e), comparable to isogenic $FtsZ^+$ strains (58 min) (Fig. 1f and Supplementary Fig. 4d). Moreover, measurement of the viable cell count (colony forming units; CFU) revealed that the cells are capable of reasonably efficient proliferation (Fig. 1g).

Time-lapse imaging was used to elucidate the formation of “coli-flower” like cells and how they divide. In the examples shown (Fig. 2a-c and Supplementary Videos 2-5) a more or less round cell expanded in two main directions to generate two new spherical areas connected by a newly formed branch (Fig. 2a, 17 to 85 min and Supplementary Video 1). Further blebs emerged from the original branch zone, leading in turn to the formation of additional new-branched spherical areas (Fig. 2a, stars and Supplementary Videos 2-3). Expansion of the spherical areas seemed to coincide with a reduction of material in the central zone, leading to an area with extensive narrow ramifications (Fig. 2a and

Supplementary Videos 2-3). Remarkably, despite the absence of an *ftsZ*-based division machine, separation-like events frequently occurred (Fig. 2 Arrows and Supplementary Videos 2-4-5). These events were observed both in branching areas (Fig. 2a, 279 min, 2b, 28-35 min and 2c, 35-45 min and 70-85 min) and at the neck of globular areas, generating more or less spherical progeny cells (Fig. 2b, 20-25 min and 2c, 55-70 min).

Whole genome sequencing of three independent *ftsZ*-less mutant strains revealed the presence of multiple differences to the parental strain (Supplementary Table 1). These mutations seemed to be of three main classes. First, all of the mutants had an inactivating mutation in either the gene (*mrcB*), for the bi-functional Penicillin Binding Protein 1B (PBP1B) or for its essential extracellular regulator LpoB[14,15]. PBP1B is partially redundant to PBP1A and is thought mainly to be concerned with wall synthesis during cell division[15,16]. Secondly, two of the mutants had (different) mutations in the gene *lpp*, which encodes the major lipoprotein Lpp (Braun's lipoprotein), which physically connects the outer-membrane to the peptidoglycan[17]. One of these mutations would delete the last four amino acids of the Lpp protein, including the Lysine that is essential for attachment to the peptidoglycan (Supplementary Table 1). Finally, all three of the mutants had diverse mutations affecting the synthesis of various extracellular polysaccharides: lipopolysaccharide, the Enterobacterial Common Antigen (ECA) or colanic acid (Supplementary Table 1).

To test which of these mutations were needed for the switch to the CFL mode of growth, we carried out genetic reconstruction experiments in which null mutations in the various genes were introduced into a *ΔftsZ* strain carrying a plasmid pOU82-*ftsZ*$^{+}$ that enables normal growth and division in the walled state. The cells were further engineered so that this plasmid could be eliminated by addition of IPTG (see Methods). As a control, IPTG was added to one of the original *ftsZ*-less walled mutant strains (*ΔftsZsup5*, bearing *mrcB* and *lpp* mutations) carrying the plasmid pOU82-*ftsZ*. The strain readily lost the plasmid (which carries a *lacZ* gene), as shown by the emergence of white colonies on X-gal plates (Lac^{-}; Fig. 3a) and loss of the *ftsZ* gene was confirmed by multiplex PCR (Supplementary Fig. 4a, line 1). In contrast, reconstructed strains bearing *ΔftsZ* and either *ΔlpoB* or *Δlpp*, showed

prolonged retention of the *ftsZ* plasmid (Fig. 3a, *ΔftsZ/Δlpp* and *ΔftsZ/ΔlpoB*; Supplementary Fig. 4a, lanes 2 and 3). Phase contrast microscopy revealed that depletion of *ftsZ* in either *ΔlpoB* or *Δlpp* mutants led to the formation of filamentous cells but not CFL-like cells (Fig. 3a). In contrast, a strain bearing both *Δlpp* and *ΔlpoB* deletions readily lost the plasmid (Fig. 3a, *ΔftsZ/Δlpp/ΔlpoB*; Supplementary Fig. 4a lane 4). Examination of its morphology revealed a CFL phenotype similar to that of the original suppressed *ftsZ* strains (Fig. 3a, lower left and right panels), thus revealing that combined disruption of the *lpoB* and *lpp* genes is sufficient to enable walled cells to tolerate loss of *ftsZ* by switching into the CFL mode of proliferation, although secondary mutations frequently arise that then enable more robust growth (Supplementary Data 1 and Fig. 4c-d). This effect was specific for the *lpoB*/PBP1B pathway because in reconstructed strains containing *ΔftsZ Δlpp* and deletions in the related *lpoA*/PBP1A pathway[15] loss of the *ftsZ* plasmid was not permitted (Supplementary Fig. 4b),

In the above reconstruction experiments it is important to note that the switch to the CFL state occurred in walled cells without going through an L-form intermediate. We also tested the genetic requirements for CFL growth starting from the L-form *ΔftsZ* state. In accordance with the above results, when L-forms bearing *ΔftsZ* and either *ΔlpoB* or *ΔmrcB* (PBP1B) were streaked in the absence of a cell wall inhibitor (no phosphomycin), but presence of an osmotic stabiliser, colonies appeared with high efficiency (Fig. 3b), suggesting an efficient conversion to the CFL state. In contrast, virtually no colonies appeared from L-forms bearing *ΔftsZ* only or *ΔftsZ* and either *ΔlpoA* or *ΔmrcA*. The strain bearing *ΔftsZ* and *Δlpp*, gave an intermediate result, suggesting that, unlike *lpoB*/*mrcB*, mutation of *lpp* is not sufficient to enable an efficient L-form to CFL transition and perhaps the acquisition of a secondary mutation is required (Fig. 3b).

To further investigate the role of these mutations (i.e. *lpoB*, *lpp* and colanic acid) in CFL growth, we introduced plasmids bearing arabinose-inducible *lpoB*, *mrcB*, *lpp* or *wcaJ* genes into either one of the spontaneously selected mutants (*ΔftsZsup5,* bearing *mrcB, lpp* and *wcaJ* mutations) or the reconstructed strain containing deletions in *ftsZ, lpp* and *lpoB* (*ΔftsZ/Δlpp/ΔlpoB*$_{sup}$). Addition of the inducer, arabinose, had no major effect on growth or

morphology for strains carrying inducible *wcaJ* or *lpp* genes (Supplementary Data 2 and Fig. 5). However, induction of *lpoB*, in the strain *ΔftsZ/Δlpp/ΔlpoB*$_{sup}$, and *mrcB*, in the strain *ΔftsZsup5,* abolished growth (Fig. 4a, +*lpoB* and 4c, +*mrcB*). (Expression of *lpoB* in an isogenic *ftsZ*$^{+}$ strain had no effect; Supplementary Fig. 6a). Phase contrast and time-lapse imaging of cells in the absence of inducer revealed the expected branching and bulging pattern of growth (Supplementary Fig. 6b and Video 6). However, the *lpoB* or *mrcB* induced cells behaved in a strikingly different manner, reverting slowly to a rod-shaped morphology, and then forming elongated filamentous cells that did not divide (Fig. 4b, d and e, Supplementary Video 7), similar to an *ftsZ* depleted, otherwise wild type strain. Thus, our results show that loss of PBP1B synthesis or activity is required for the CFL mode of cell growth but that *lpp* or *wcaJ* lesions are less or not important. Additionally, we also showed that the cell wall elongation system is required for CFL growth (Supplementary Data 3 and Fig. 7).

To our knowledge, this is the first report of growth and viability of a walled *E. coli ftsZ* null mutant, after 35 or so years of study. It seems likely that several labs will have had the need or opportunity to attempt to generate such mutants but because effective suppression in the walled state requires two or more independent mutations, the frequency at which viable mutants would occur would normally be extremely low. Our ability to isolate such a mutant emerged by studying L-form (wall-free) bacteria, which use a Z-ring-independent means of proliferation[4,6]. This illustrates the power of the L-form system for studying the fundamental processes of cell wall synthesis and cell division.

We have also not been able to find previous reports of the strange CFL cell morphology. The dramatic morphological transition requires inactivation of both FtsZ and PBP1B. The lethality that occurs when *lpoB* or *mrcB* are reactivated in CFL strains (Fig. 4) appears to be associated with reversion to a more regular rod-shaped morphology. We suppose that the relatively constant cell diameter associated with rod-shaped growth is incompatible with the ability of *ftsZ* deficient cells to divide. Indeed, CFL cells seem to undergo division at deeply pinched sites either in narrow tubes or at the junctions between

bulbous cell structures. If so, the role of the PBP1B lesion would be to block the cylindrical extending mode of cell growth, and or enable the bulging, branching mode of growth. The efficiency of CFL growth and transition into this state seems to be sensitive to the presence of a range of additional mutations, including *lpp* and various extracellular polymers. Further work will be needed to dissect the roles of these factors.

Although lacking the normal cell division machinery, these *E. coli ftsZ*-less mutants divide efficiently (Fig. 1f-g), suggesting the existence of an effective mode of cell-cell separation in absence of *ftsZ*. The vast majority of known bacteria seem to rely on the FtsZ-based division machinery for proliferation and, usually, for viability. However, there are striking examples among both pathogens (e.g. chlamydia) and free-living bacteria (e.g. *Planctomyces*), that have dispensed with FtsZ. Phylogenetic trees suggest strongly that these organism are descended from bacteria that once possessed FtsZ. Our results demonstrate that only one or two mutations are needed to enable a dramatic evolutionary switch from dependence to independence of the Z ring machine and highlight the extraordinary evolutionary adaptability of the bacteria.

References

1 Schneider, T. & Sahl, H. G. Lipid II and other bactoprenol-bound cell wall precursors as drug targets. *Curr Opin Investig Drugs* **11**, 157-164, (2010).

2 Errington, J. L-form bacteria, cell walls and the origins of life. *Open Biol* **3**, 120143, (2013).

3 Typas, A., Banzhaf, M., Gross, C. A. & Vollmer, W. From the regulation of peptidoglycan synthesis to bacterial growth and morphology. *Nat Rev Microbiol* **10**, 123-136, (2012).

4 Leaver, M., Domínguez-Cuevas, P., Coxhead, J. M., Daniel, R. A. & Errington, J. Life without a wall or division machine in *Bacillus subtilis*. *Nature* **457**, 849-853, (2009).

5 Mercier, R., Domínguez-Cuevas, P. & Errington, J. Crucial role for membrane fluidity in proliferation of primitive cells. *Cell Rep* **1**, 417-423, (2012).

6 Mercier, R., Kawai, Y. & Errington, J. General principles for the formation and proliferation of a wall-free (L-form) state in bacteria. *Elife* **3**, (2014).

7 Pilhofer, M. *et al.* Discovery of chlamydial peptidoglycan reveals bacteria with murein sacculi but without FtsZ. *Nat Commun* **4**, 2856, (2013).

8 Liechti, G. W. *et al.* A new metabolic cell-wall labelling method reveals peptidoglycan in *Chlamydia trachomatis*. *Nature* **506**, 507-510, (2014).

9 Jeske, O. *et al. Planctomycetes* do possess a peptidoglycan cell wall. *Nat Commun* **6**, 7116, (2015).

10 Kawai, Y., Mercier, R. & Errington, J. Bacterial cell morphogenesis does not require a preexisting template structure. *Curr Biol* **24**, 863-867, (2014).

11 Ranjit, D. K. & Young, K. D. The Rcs stress response and accessory envelope proteins are required for de novo generation of cell shape in *Escherichia coli*. *J Bacteriol* **195**, 2452-2462, (2013).

12 Billings, G. *et al.* De novo morphogenesis in L-forms via geometric control of cell growth. *Molecular Microbiology* **93**, 883-896, (2014).

13 Dai, K. & Lutkenhaus, J. *ftsZ* is an essential cell division gene in *Escherichia coli*. *J Bacteriol* **173**, 3500-3506, (1991).

14 Paradis-Bleau, C. *et al.* Lipoprotein cofactors located in the outer membrane activate bacterial cell wall polymerases. *Cell* **143**, 1110-1120, (2010).

15 Typas, A. *et al.* Regulation of peptidoglycan synthesis by outer-membrane proteins. *Cell* **143**, 1097-1109, (2010).

16 Gray, A. N. *et al.* Coordination of peptidoglycan synthesis and outer membrane constriction during *Escherichia coli* cell division. *Elife* **4**, (2015).

17 Braun, V. & Bosch, V. Repetitive sequences in the murein-lipoprotein of the cell wall of *Escherichia coli*. *Proc Natl Acad Sci U S A* **69**, 970-974, (1972).

Acknowledgements

We thank Tâm Mignot for hosting parts of the work in his laboratory, Waldemar Vollmer for the gift of the plasmid pBAD33-*lpoB* and comments on the manuscript, Henrik Strahl and Leon Espinosa for helpful discussion. This work was funded by European Research Council Advanced Investigator Grants (# 250363 and # BH141574) to JE.

Author contributions

R.M. designed the experiments. R.M. performed the experiments. R.M. and Y.K. analysed the data. R.M. and J.E. wrote the manuscript.

Competing Financial interests

The authors declare no competing financial interests

Figure Legends

Figure 1: Isolation and characterisation of walled *Escherichia coli ftsZ*-less strains

a, Summary of the morphological transitions described in the paper.

b, Cell wall reversion of *E. coli* L-form strains wild type (TB28, top left) and RM349 (*ΔftsZ,* bottom left), following removal of the PG precursor synthesis inhibitor fosfomycin. Cells were cultured on L-form-supporting medium (NA + MSM) plates (left). Representative phase contrast images (right) show cell wall reverted *E. coli* wild type (top) and RM349 (bottom) cells after 12h incubation.

c, Growth of the strain *ΔftsZsup5* on NA+ 20 mM Mg^{2+} plates with or without 10 µg/ml of Ampicillin, as indicated.

d, Phase contrast microscopy of cells of three independent *ΔftsZsup* strains grown in NB with 20 mM Mg^{2+}.

e, Phase contrast microscopy of the *ΔftsZsup5* cells grown in NB with 20 mM Mg^{2+}*,* after reintroduction of the plasmid pOU82-*ftsZ*.

f, Growth profile of the strain *ΔftsZsup5,* in presence (blue) or absence (red) of the plasmid pOU82-*ftsZ,* in NB with Mg^{2+}. The mass doubling time calculated for the strain *ΔftsZsup5* is about 58 min in presence and 60 min in the absence of FtsZ.

g, Colony-forming units of the strain *ΔftsZsup5,* grown in the presence (blue) or absence (red) of the plasmid pOU82-*ftsZ,* corresponding to the growth profile from **f**.

Scale bars, 3 µm.

Figure 2: Time lapse imaging of a CFL strain grown in the complete absence of FtsZ

a-c, *E. coli ΔftsZsup* strains grown in NB with 20 mM Mg^{2+} were observed by time-lapse phase contrast microscopy. Elapsed time (min) is shown in each panel. Scale bars, 3 µm. Stars identify blebs emerging from the original branch zone and arrows point to division events.

Figure 3: PBP1B activity inactivation is required for the transition to a CFL mode of proliferation in the absence of FtsZ

a, *ftsZ* loss assays (top) of RM446 (*ΔftsZsup5*), RM411 (*ΔftsZ/ΔlpoB*), RM413 (*ΔftsZ/Δlpp*) and RM419 (*ΔftsZ/Δlpp/ΔlpoB*) strains, containing the plasmids pOU82-*ftsZ* and pKG339. Walled cells were streaked on NA plates with 20mM Mg^{2+}, Tetracycline, IPTG and Xgal. The loss of *ftsZ* results in the formation of white colonies, which was verified by multiplex PCR (Supplementary Fig 4a). Corresponding cell morphologies (bottom) of the different streaked strains were imaged by phase contrast microscopy.

b, Cell wall reversion of *E. coli* L-form strains RM349 (*ΔftsZ*), RM411 (*ΔftsZ/ΔlpoB*), RM451 (*ΔftsZ/ΔmrcB*), RM413 (*ΔftsZ/Δlpp*), RM453 (*ΔftsZ/ΔlpoA*) and RM452 (*ΔftsZ/ΔmrcA*) lacking pOU82-*ftsZ*, following removal of the PG precursor synthesis inhibitor fosfomycin. Cells were cultured on L-form-supporting medium (NA + MSM) plates.

Figure 4: PBP1B activity inhibits CFL proliferation by restoration of cylindrical cell shape morphology in the absence of FtsZ

a, Growth of the strain RM445 (*ΔftsZ/Δlpp/ΔlpoB*$_{sup}$), carrying the plasmid pBAD33-*lpoB,* streaked on NA + 20 mM Mg^{2+} plates in absence (left) or presence (right) of the inducer for *lpoB* expression (Arabinose).

b, Phase contrast microscopy of RM445 (*ΔftsZ/Δlpp/ΔlpoB*$_{sup}$) pBAD33-*lpoB* cells from **b** in the presence of arabinose.

c, Growth of the strain RM362 (*ΔftsZsup5),* carrying the plasmid pBAD33-*mrcB,* streaked on NA + 20 mM Mg^{2+} plates in absence (left) or presence (right) of the inducer for *mrcB* expression inducer (Arabinose).

d, Phase contrast microscopy of RM362 cells (*ΔftsZsup5),* carrying pBAD33-*mrcB* from **c** in the presence of arabinose.

e, Strain RM445 (*ΔftsZ/Δlpp/ΔlpoB*$_{sup}$), carrying the plasmid pBAD33-*lpoB,* grown on NA/Mg^{2+} with arabinose, was observed by time-lapse phase contrast microscopy. Elapsed time (min) is shown in each panel.

Scale bars, 3 μm.

Methods

Bacterial strains, plasmids and growth conditions

The bacterial strains and plasmids constructs used in this study are shown in Supplementary Table 3. DNA manipulations, *E. coli* DH5α transformation and P1 phage transduction were carried out using standard methods[18]. Briefly, the plasmid pOU82-*Cm-ftsZ* was constructed by insertion, by the Lambda Red recombinase system[19], of the chloramphenicol cassette from pKD3 into pOU82-*Amp-ftsZ*. The plasmids pBAD33-*lpp*, pBAD33-*wcaJ and* pBAD33-*mrcB* were constructed by insertion of the coding sequences of the *lpp*, *wcaJ and mrcB* genes into pBAD33 digested by the restriction enzymes KpnI and HindIII or XbaI. The plasmid pBAD24-*lpp* was constructed by insertion of the coding sequence of the *lpp* into pBAD24 digested by the restriction enzymes EcoRI and HindIII. *E. coli* L-forms were prepared and grown, as previously described[6], in osmoprotective medium composed of 2 x

316 MSM media pH 7 (40 mM $MgCl_2$, 1 M sucrose and 40 mM maleic acid) mixed 1:1 with 2 x
317 NBA (Nutrient Broth with 2% Agar (Oxoid)) in presence of fosfomycin (FOS) at 0.4 mg/ml. *E.*
318 *coli* CFL mutant strains were firstly selected on MSM/NBA and then further cultured on
319 Nutrient Broth (NB, Oxoid) or Nutrient Broth 1% Agar in the presence of 20 mM $MgCl_2$.
320 Unless specified, the various *E. coli* strains are incubated at 30°C. When necessary,
321 antibiotics and supplements were added to media at the following concentrations: ampicillin,
322 10 or 100 µg/ml; mecillinam, 5 µg/ml; aztreonam, 0.05 µg/ml; A22 (sigma), 10 µg/ml
323 chloramphenicol, 25 µg/ml; kanamycin, 25 µg/ml; tetracycline, 10 µg/ml; spectinomycin, 50
324 µg/ml; $MgCl_2$, various concentrations; arabinose, 0.2 %; glucose, 0,5%; Sodium Dodecyl
325 Sulfate (SDS), 0,5%; IPTG, 1 mg/ml and X-gal, 4%.
326

327 **Plasmid pOU82-*ftsZ* loss assay**

328 Various *E. coli* strains bearing the plasmid pOU82-*ftsZ* were transformed with the plasmid
329 pKG339[20] and plated on NA with tetracycline at 30°C for 3 days. Strains carrying both
330 plasmids were streaked on NA plates with 20mM Mg^{2+}, Tetracycline, IPTG and X-gal and
331 incubated at 30°C for 3-4 days. White colonies were streaked on NA plates with 20 mM Mg^{2+}
332 and X-gal.

333 **Transformation of *E. coli ftsZ*-less strains**

334 A 1 ml sample of an overnight culture of an *E. coli* CFL strain was suspended in 200 µl of
335 TSB, containing 20 % glycerol, 10 % PEG (MW 3350), 5 % DMSO, 10 mM $Mgcl_2$, 10 mM
336 $MgSO_4$ in NB. A plasmid of interest was added and incubated on ice for 30 min. After heat
337 shock at 37°C for 5 min, 1 ml of NB with 20 mM $Mgcl_2$ was added and the sample was
338 incubated for 30 min at 30°C. The sample was plated on NB 1% Agar with 20 mM $Mgcl_2$ and
339 the appropriate antibiotic and incubated at 30°C.

Multiplex PCR

Mutiplex PCR was performed as described by[6]. Briefly, *E. coli* genomic DNA was purified using a standard phenol-chloroform extraction protocol. The primers were designed using MPprimer software[21] and the recommended procedure was used for the PCR reaction.

Genome sequencing and SNPs identification

Whole genome sequencing was performed with the Illumina HiSeq 2000 System (GATC-Biotech, Germany). Sequencing samples were prepared using a standard chloroform/phenol extraction procedure. Sequence reads were aligned with CLC Workbench (CLC Bio-Qiagen, Aarhus, Denmark) software using the NCBI *E. coli* MG1655 genome (GenBank: U00096.3) as reference. SNPs and deletion/insertion were also analysed with the CLC Workbench software.

Microscopy and image analysis

For snap-shot and time-lapse microscopy, exponentially growing cultures of the different CFL walled strains were mounted and sealed on microscope slides covered with a thin film of 1% agarose, in NB containing 20mM magnesium. Antibiotics, DAPI and arabinose were added in the agar pad, as necessary. The cells were imaged for snap-shot microscopy on a Zeiss Axiovert 200M (Zeiss ×100 Plan-Neofluar oil immersion objective) microscope, and for time-lapse microscopy, on a Nikon Eclipse Ti (Nikon × 100 Plan Fluor oil immersion objective) contained in a temperature control chamber at 30°C. Images were acquired with Metamorph 6 (Molecular Devices). Pictures and movies were prepared for publication using ImageJ (http://rsb.info.nih.gov/ij) and Adobe Photoshop.

Method references

18 Sambrook, J., Fritsch, E.F., and Maniatis, T. Molecular Cloning: A Laboratory Manual. *Cold Spring Harbor: Cold Spring Harbor Laboratory Press*, (1989).

19 Datsenko, K. A. & Wanner, B. L. One-step inactivation of chromosomal genes in *Escherichia coli* K-12 using PCR products. *Proc Natl Acad Sci U S A* **97**, 6640-6645, (2000).

20 Jensen, R. B., Grohmann, E., Schwab, H., Diaz-Orejas, R. & Gerdes, K. Comparison of *ccd* of F, *parDE* of RP4, and *parD* of R1 using a novel conditional replication control system of plasmid R1. *Mol Microbiol* **17**, 211-220, (1995).

21 Shen, Z. *et al.* MPprimer: a program for reliable multiplex PCR primer design. *BMC Bioinformatics* **11**, 143, (2010).

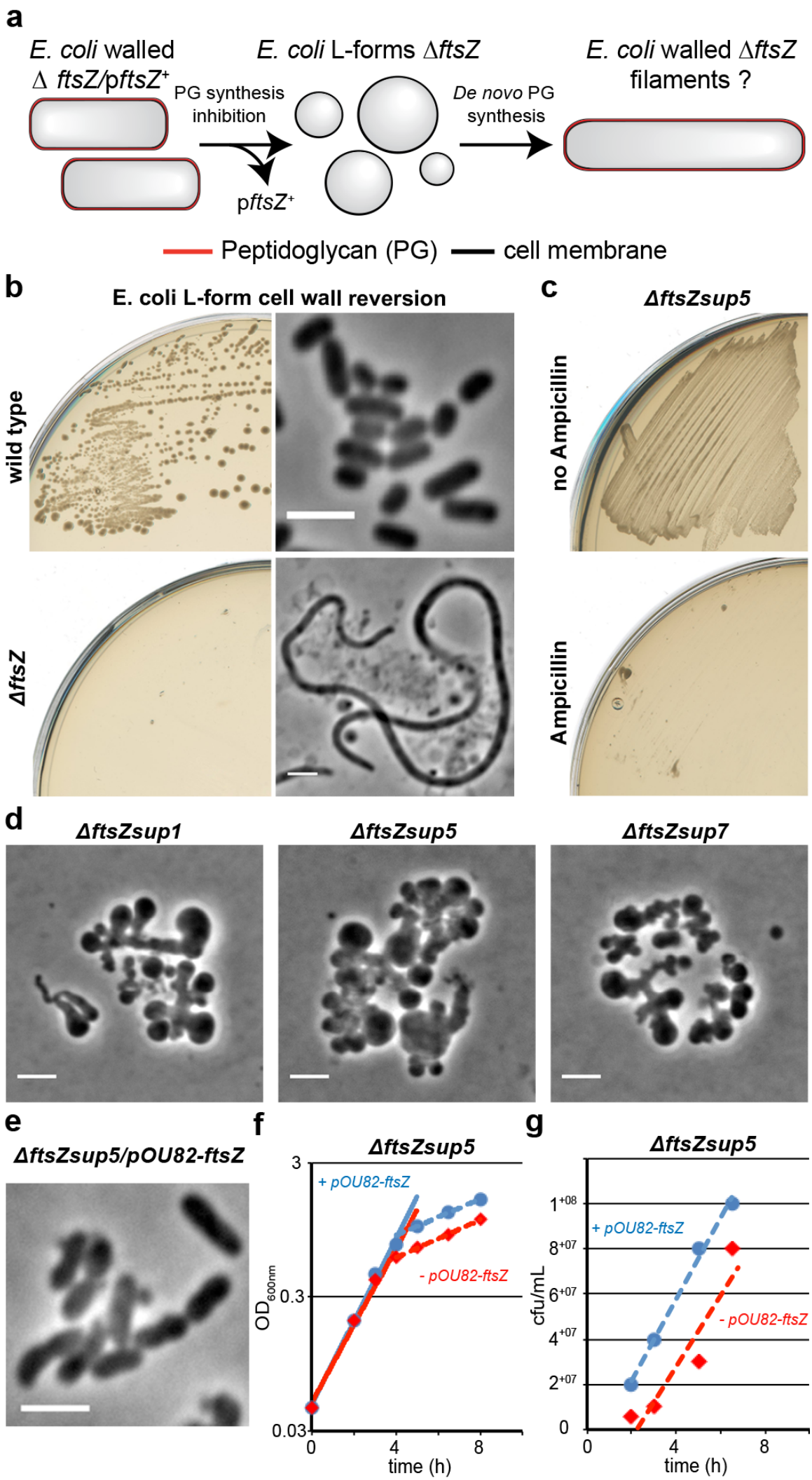
a
E. coli walled
Δ ftsZ/pftsZ+
PG synthesis inhibition
pftsZ+
E. coli L-forms ΔftsZ
De novo PG synthesis
E. coli walled ΔftsZ filaments ?
Peptidoglycan (PG)
cell membrane
b
E. coli L-form cell wall reversion
wild type
ΔftsZ
c
ΔftsZsup5
no Ampicillin
Ampicillin
d
ΔftsZsup1
ΔftsZsup5
ΔftsZsup7
e
ΔftsZsup5/pOU82-ftsZ
f
ΔftsZsup5
+ pOU82-ftsZ
- pOU82-ftsZ
OD600nm
3
0.3
0.03
0
4
8
time (h)
g
ΔftsZsup5
+ pOU82-ftsZ
- pOU82-ftsZ
cfu/mL
1+08
8+07
6+07
4+07
2+07
0
4
8
time (h)

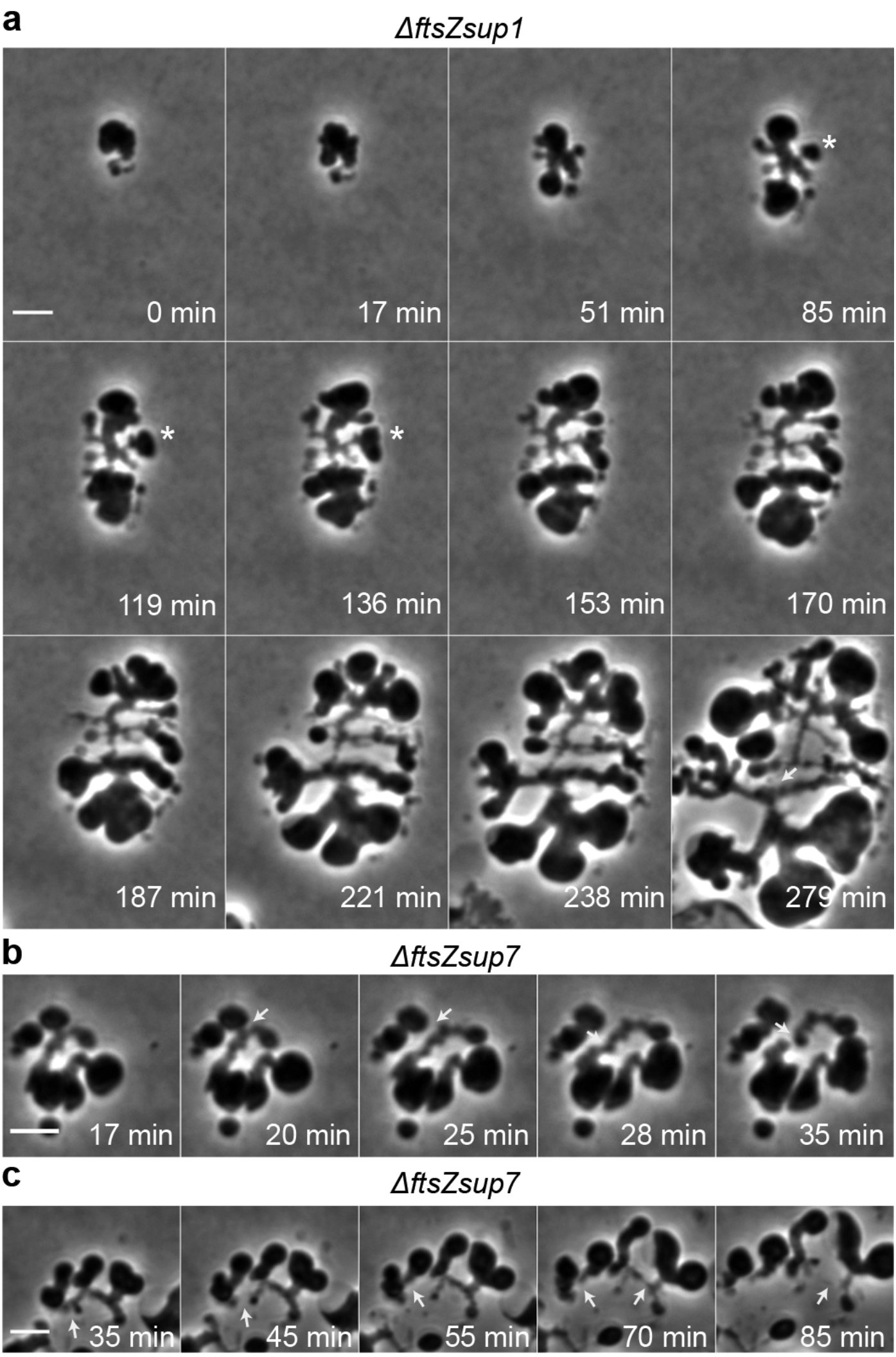
a
ΔftsZsup1
0 min
17 min
51 min
85 min
119 min
136 min
153 min
170 min
187 min
221 min
238 min
279 min
b
ΔftsZsup7
17 min
20 min
25 min
28 min
35 min
c
ΔftsZsup7
35 min
45 min
55 min
70 min
85 min

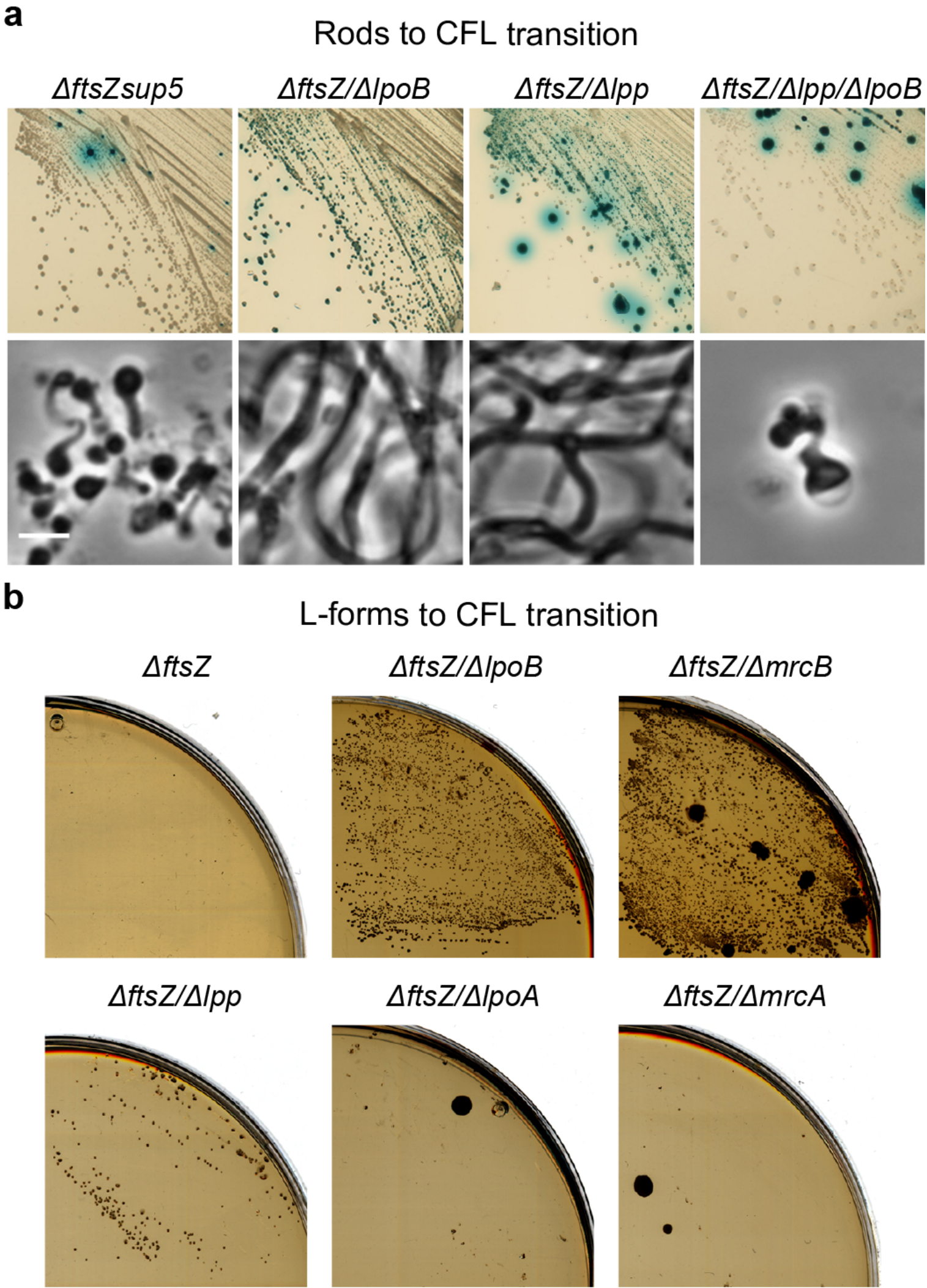
a
Rods to CFL transition
ΔftsZsup5
ΔftsZ/ΔlpoB
ΔftsZ/Δlpp
ΔftsZ/Δlpp/ΔlpoB
b
L-forms to CFL transition
ΔftsZ
ΔftsZ/ΔlpoB
ΔftsZ/ΔmrcB
ΔftsZ/Δlpp
ΔftsZ/ΔlpoA
ΔftsZ/ΔmrcA

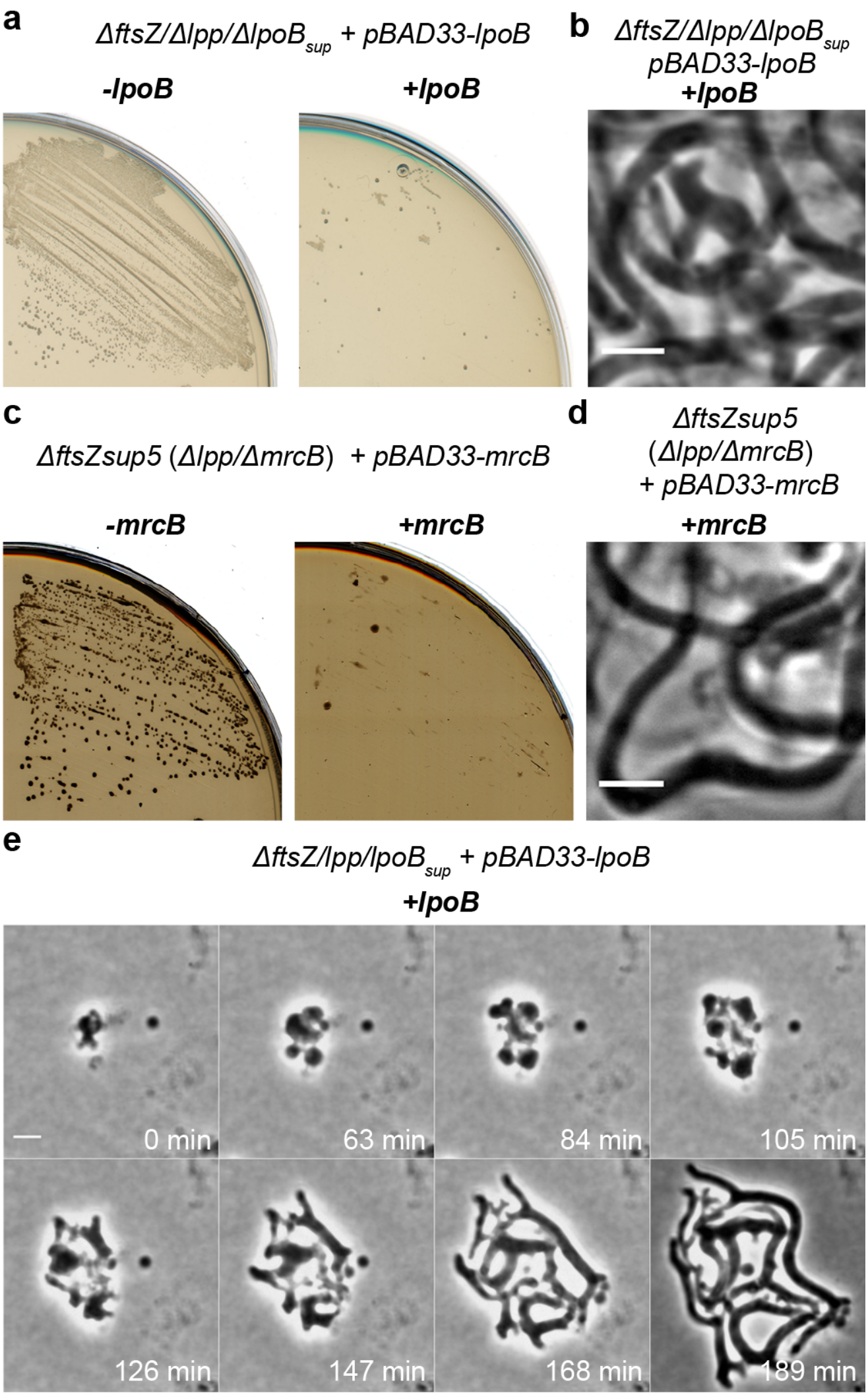
a
ΔftsZ/Δlpp/ΔlpoB$_{sup}$ + pBAD33-lpoB
-lpoB
+lpoB
b
ΔftsZ/Δlpp/ΔlpoB$_{sup}$
pBAD33-lpoB
+lpoB
c
ΔftsZsup5 (Δlpp/ΔmrcB) + pBAD33-mrcB
-mrcB
+mrcB
d
ΔftsZsup5
(Δlpp/ΔmrcB)
+ pBAD33-mrcB
+mrcB
e
ΔftsZ/lpp/lpoB$_{sup}$ + pBAD33-lpoB
+lpoB
0 min
63 min
84 min
105 min
126 min
147 min
168 min
189 min

Supplementary Information

Supplementary Data

Supplementary Data 1: Spontaneous mutations arise in CFL selective conditions

It appears that secondary mutations frequently arise in CFL selective conditions, presumably to improve the efficiency of growth. We sequenced a variant of the *ΔftsZ/Δlpp/ΔlpoB* strain that showed improved growth, giving a mass doubling time of 60 min, similar to that of the original *ftsZsup* strains (Supplementary Fig. 4c-d, *ΔftsZ/Δlpp/ΔlpoB*$_{sup}$). As for the original CFL mutants, we found a mutation affecting colanic acid synthesis (truncation of the *wzxC* and *wcaJ* genes; Supplementary Table 2). It therefore seems that synthesis of colanic acid directly or indirectly impairs the growth of these complex suppressed strains, for reasons that we have not yet determined. It is interesting to note that colanic acid is normally made under stress conditions [1] and that mutations affecting colanic acid synthesis have been found in at least one well characterised L-form strain [2].

Supplementary Data 2: Effects of the overexpression of Lpp in the *ΔftsZ/Δlpp/ΔlpoB*$_{sup}$ strain on SDS sensitivity and on CFL proliferation

We firstly tested if the levels of *lpp* expression from plasmids pBAD33 (pACYC184) or pBAD24 (pBR322) were sufficient to complement the known sensitivity of an *lpp* mutant to SDS (Supplementary Fig 5a). As shown in Supplementary Fig 5b, in the presence of the *lpp* inducer arabinose the plasmid pBAD24-*lpp,* but not pBAD33-*lpp,* can complement the sensitivity to 0.5% SDS of the ΔftsZ/Δlpp/ΔlpoBsup (FtsZ+) strain, suggesting that the level of *lpp* expression from pBAD24 was sufficient to complement an *lpp* mutation. We have secondly transformed both plasmids, pBAD33-*lpp* and pBAD24-*lpp,* into the CFL (FtsZ$^-$) *ΔftsZsup5* and/or *ΔftsZ*/*Δlpp*/*ΔlpoB*$_{sup}$ strains. As shown in Supplementary Fig 5c to h, no effect on CFL growth or morphology was observed upon induction of *lpp* expression (Arabinose).

Supplementary Data 3: Cell wall elongation system is required for CFL growth

We anticipated that the cell wall elongation system would be required for CFL growth, and indeed, as shown in Supplementary Fig 7a-b (right panels), inhibition of MreB or PBP2 function with specifically targeted antibiotics (A22 and mecillinam, respectively) blocked CFL proliferation. Controls showed that growth inhibition by these antibiotics could be restored by overexpression of *ftsQAZ* (ftsZup), as described previously [3]. Finally, we also tested inhibition of PBP3 activity. Surprisingly, given that this protein is part of the *ftsZ*-dependent division machinery [4], this resulted in loss of CFL proliferation (Supplementary Fig. 7c), for reasons that are not yet clear.

Supplementary Figures

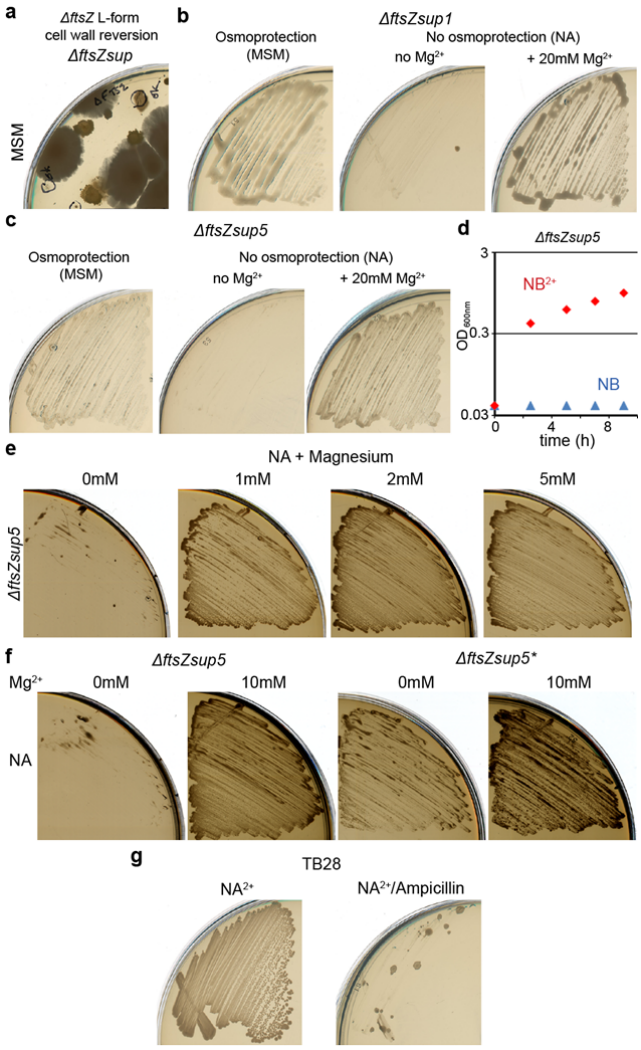

Supplementary Figure 1: Characterisation of walled *E. coli ftsZ*-less strains

a, Cell wall reversion of *E. coli* L-form strain RM349 (*ΔftsZ*), upon removal of the PG precursor synthesis inhibitor fosfomycin, on L-form-supporting medium (NA + MSM) plates after two weeks at 30°C.

b-c, Growth of the strain *ΔftsZsup1* (**b**) and *ΔftsZsup5* (**c**) streaked on L-form-supporting medium (NA + MSM, left) or NA in the absence (no Mg^{2+}, middle) or presence (20 mM Mg^{2+}, right) of 20 mM magnesium.

d, Growth profile of the strain *ΔftsZsup5* in NB in the presence (red, NB^{2+}) or absence (blue, NB) of 20 mM Mg^{2+}.

e, Growth of the strain *ΔftsZsup5* streaked on NA plates with various concentration of Mg^{2+}.

f, Growth of the strain *ΔftsZsup5* (left panels) and *ΔftsZsup5**, magnesium dependant suppressor (right panels) streaked on NA plates in absence (0 mM) or presence (10 mM) of 10 mM magnesium.

g, Growth of the strain wild type TB28 streaked on NA + 20 mM Mg^{2+} plates with (NA^{2+}/Ampicillin) or without (NA^{2+}) 10 µg/ml of Ampicillin.

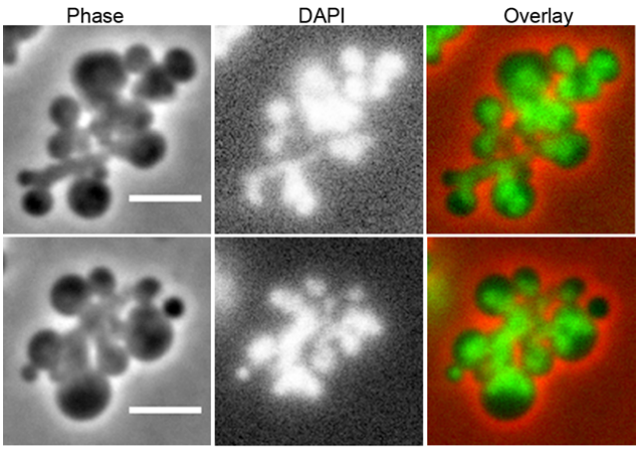

Supplementary Figure 2: Nucleoid localisation in an *E. coli ftsZ*-less strain

Phase contrast (Phase, left) and fluorescence (DAPI, middle) microscopy of *ΔftsZsup*5 cells grown in NB with Mg^{2+} and stained with DAPI. Overlay (right) represents the merge of phase and fluorescent images. Scale bar, 3 µm.

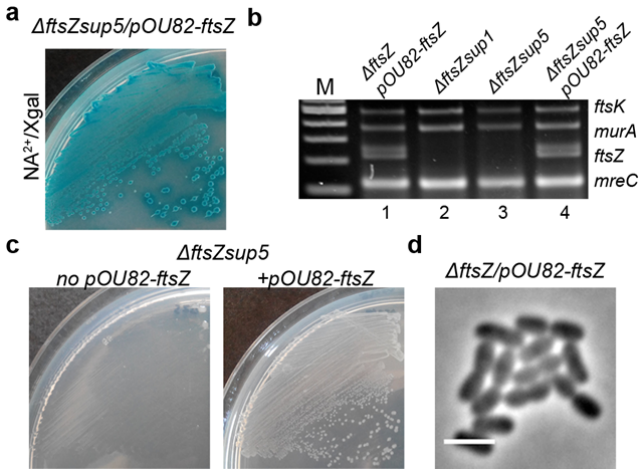

Supplementary Figure 3: Growth and cell morphology after reintroduction of *ftsZ* in an *E. coli ftsZ*-less strain.

a, Growth of the strain *ΔftsZsup5,* after reintroduction of the plasmid pOU82-*ftsZ,* streaked on NA + 20 mM Mg^{2+} plate, containing X-gal to show the presence of the plasmid.

b, Multiplex PCR of the *ftsK*, *murA*, *ftsZ* and *mreC* genes from genomic DNA of the *E. coli* strains *ΔftsZ* pOU82-*ftsZ* (1), *ΔftsZsup1* (2), *ΔftsZsup5* (3) and *ΔftsZsup5* pOU82-*ftsZ* (4). M represents the DNA ladder.

c, Growth of the strain *ΔftsZsup5,* streaked on NA with no added magnesium with (right) or without (left) the plasmid pOU82-*ftsZ.*

d, Phase contrast microscopy of the *ΔftsZ* cells, carrying the plasmid pOU82-*ftsZ,* grown in NB with 20 mM Mg^{2+}. Scale bar, 3 μm.

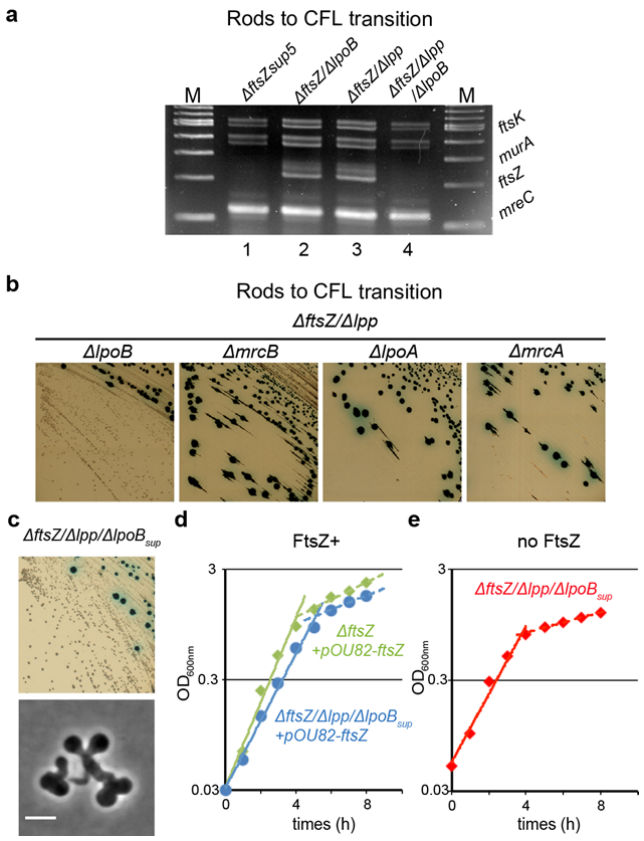

Supplementary Figure 4: Loss of Lpp and PBP1B activities promotes an *ftsZ*-less but walled mode of proliferation.

a, Multiplex PCR of the *ftsK*, *murA*, *ftsZ* and *mreC* genes from genomic DNA of the *E. coli* strains *ΔftsZsup5* (1), *ΔftsZ/Δlpp* (2), *ΔftsZ/ΔlpoB* (3) and *ΔftsZ/Δlpp/ΔlpoB* (4) obtained from the plates in Figure 3a. M represents the DNA ladder.

b, *ftsZ* loss assays of RM119 (*ΔftsZ/Δlpp/ΔlpoB*), RM448 (*ΔftsZ/Δlpp/ΔmrcB*), RM450 (*ΔftsZ/Δlpp/ΔlpoA*), RM449 (*ΔftsZ/Δlpp/ΔmrcA*) strains, containing the plasmids pOU82-*ftsZ* and pKG339, streaked on NA containing 20mM Mg^{2+}, Tetracycline, IPTG and Xgal.

c, *ftsZ* loss assay (top) of RM447 (*ΔftsZ/Δlpp/ΔlpoB*$_{sup}$) strain, containing the plasmids pOU82-*ftsZ* and pKG339, streaked on NA containing 20 mM Mg^{2+}, Tetracycline, IPTG and Xgal. Corresponding cell morphology (bottom) of the streaked strain was visualised by phase contrast microscopy. Scale bar, 3 µm.

d, Growth profile of strains RM349 (*ΔftsZ pOU82-ftsZ*, green) and RM447 (*ΔftsZ/Δlpp/ΔlpoB*$_{sup}$ pOU82-*ftsZ*, blue) in NB containing 20 mM Mg^{2+}. The mass doubling times calculated for strains RM349 and RM447 were about 47 and 58 min, respectively.

e, Growth profile of the strain RM445 (*ΔftsZ/Δlpp/ΔlpoB*$_{sup}$) in NB with 20 mM Mg^{2+}. The mass doubling time calculated was 60 min.

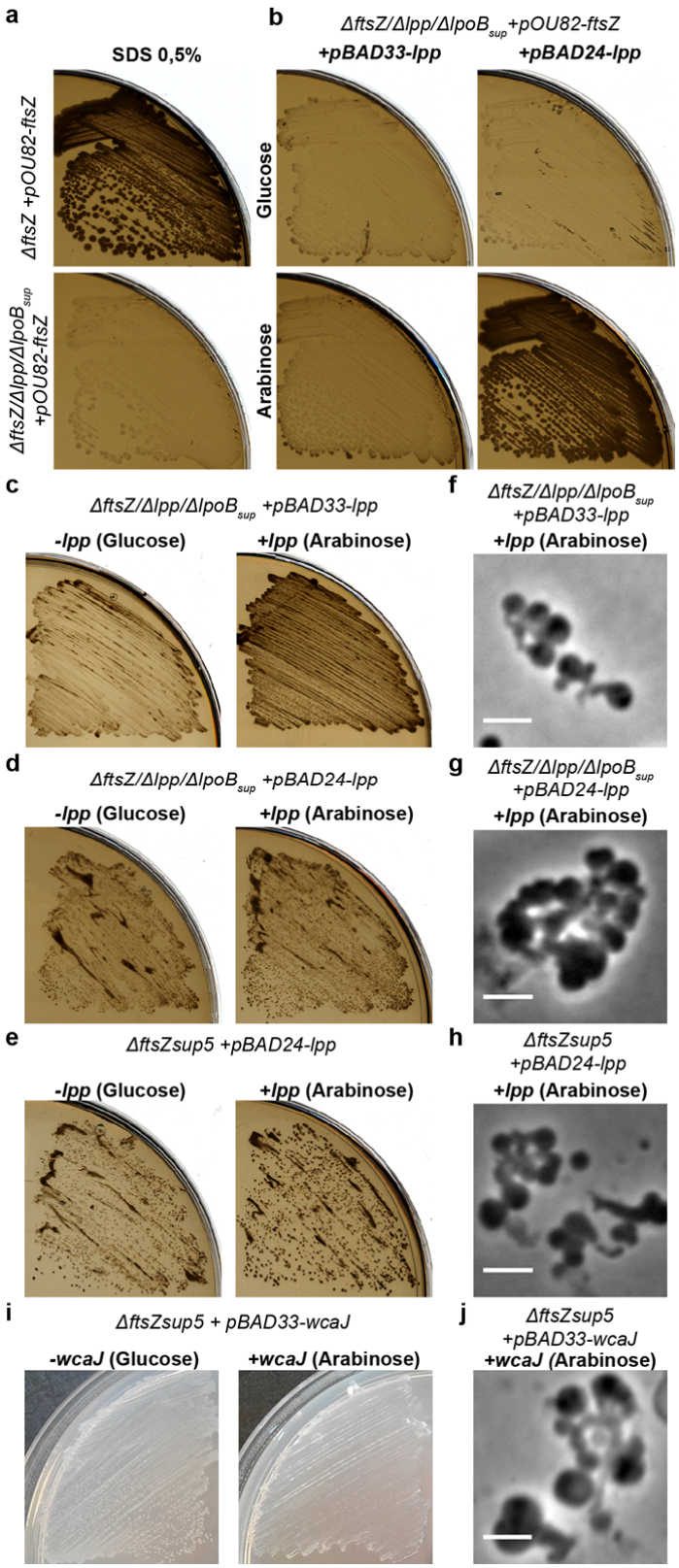
a
b
ΔftsZ/Δlpp/ΔlpoB$_{sup}$+pOU82-ftsZ
SDS 0,5%
+pBAD33-lpp
+pBAD24-lpp
ΔftsZ +pOU82-ftsZ
Glucose
ΔftsZ/Δlpp/ΔlpoB$_{sup}$ +pOU82-ftsZ
Arabinose
c
ΔftsZ/Δlpp/ΔlpoB$_{sup}$ +pBAD33-lpp
-lpp (Glucose)
+lpp (Arabinose)
f
ΔftsZ/Δlpp/ΔlpoB$_{sup}$ +pBAD33-lpp
+lpp (Arabinose)
d
ΔftsZ/Δlpp/ΔlpoB$_{sup}$ +pBAD24-lpp
-lpp (Glucose)
+lpp (Arabinose)
g
ΔftsZ/Δlpp/ΔlpoB$_{sup}$ +pBAD24-lpp
+lpp (Arabinose)
e
ΔftsZsup5 +pBAD24-lpp
-lpp (Glucose)
+lpp (Arabinose)
h
ΔftsZsup5 +pBAD24-lpp
+lpp (Arabinose)
i
ΔftsZsup5 + pBAD33-wcaJ
-wcaJ (Glucose)
+wcaJ (Arabinose)
j
ΔftsZsup5 +pBAD33-wcaJ
+wcaJ (Arabinose)

Supplementary Figure 5: Lpp or WcaJ activities do not affect CFL proliferation

a, Growth of strains RM349 (*ΔftsZ pOU82-ftsZ*, top) and RM447 (*ΔftsZ/Δlpp/ΔlpoB*$_{sup}$ pOU82-*ftsZ*, bottom) streaked on NA + 20 mM Mg^{2+} in the presence of 0.5% SDS

b, Growth of the strain RM447 (*ΔftsZ/Δlpp/ΔlpoB*$_{sup}$ pOU82-*ftsZ*), carrying plasmids pBAD33-*lpp* (left) and pBAD24-*lpp* (bottom) streaked on NA + 20 mM Mg^{2+} with 0.5% SDS, and with *lpp* expression repressed (glucose, top) or induced (arabinose, bottom).

c-e, Growth of strains RM445 (*ΔftsZ/Δlpp/ΔlpoB*$_{sup}$), carrying plasmids pBAD33-*lpp* (c) or pBAD24-*lpp* (d) and RM362 (*ΔftsZsup5*), carrying the plasmid pBAD24-*lpp* (e), streaked on NA + 20mM Mg^{2+} with *lpp* expression repressed (glucose, left) or induced (arabinose, right).

f-h, Corresponding phase contrast images of RM445 (*ΔftsZ/Δlpp/ΔlpoB*$_{sup}$) pBAD33-*lpp* (f), RM445 (*ΔftsZ/Δlpp/ΔlpoB*$_{sup}$) pBAD24-*lpp* (g) and RM362 (*ΔftsZsup5*) pBAD24-*lpp* cells from **c-e**, respectively, in the presence of inducer (arabinose).

i, Growth of strain RM362 (*ΔftsZsup5*), carrying the plasmid pBAD33-*wcaJ,* streaked on NA+ 20 mM Mg^{2+} with *wcaJ* expression repressed (glucose) or induced (arabinose).

j, Phase contrast microscopy of RM362 cells (*ΔftsZsup5*), carrying pBAD33-*wcaJ* from panel **i** in the presence of inducer (arabinose). Scale bar, 3 μm.

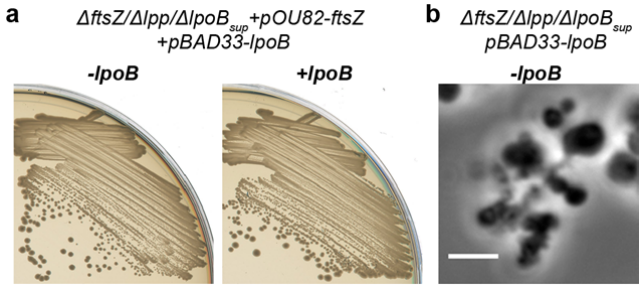

Supplementary Figure 6: PBP1B activity inhibits CFL proliferation in the absence of FtsZ

a, Growth of the strain RM445 (*ΔftsZ/Δlpp/ΔlpoB*$_{sup}$) in presence of pOU82-*ftsZ*, carrying the plasmid pBAD33-*lpoB,* streaked on NA + 20 mM Mg^{2+} in the absence (left) or presence (right) of the inducer of *lpoB* expression (arabinose).

b, Phase contrast microscopy of RM445 cells from Figure 3b in the absence of arabinose. Scale bar, 3 μm.

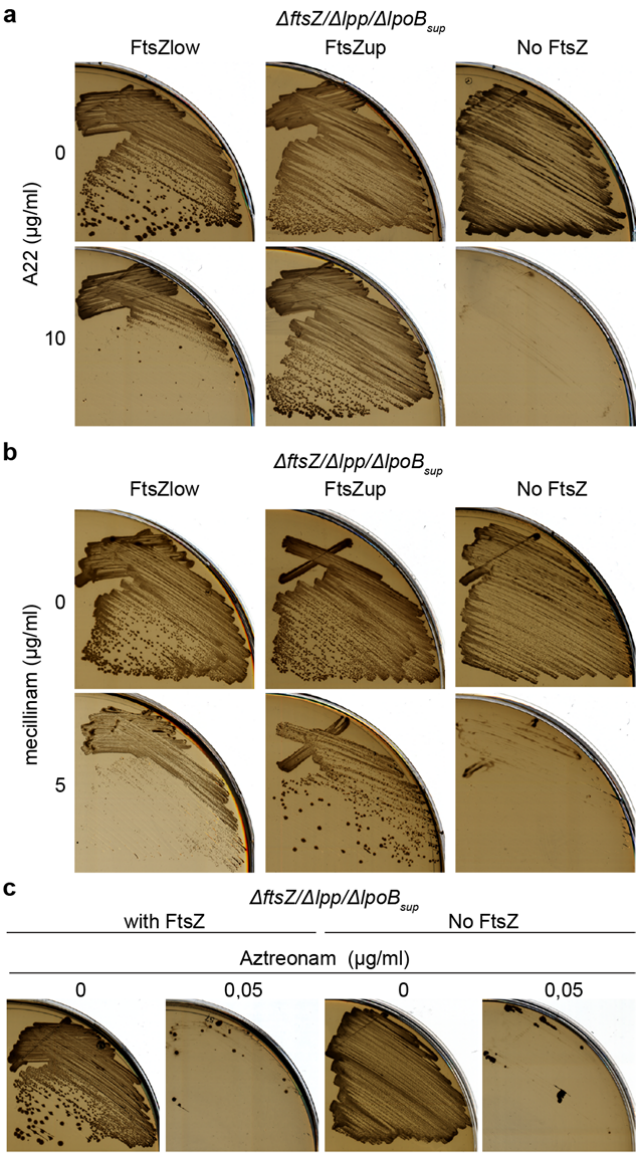

Supplementary Figure 7: Effect of the inhibition of MreB, PBP2 and PBP3 on CFL proliferation

a, Growth of the strain RM445 (*ΔftsZ/Δlpp/ΔlpoB*$_{sup}$) carrying plasmids pOU82-ftsZ (FtsZlow, left), pBS58 (FtsZup, middle) or none (No FtsZ, right), streaked on NA + 20mM Mg^{2+} in the absence (top) or presence (bottom) of 10 µg/ml of A22.

b, As **a**, but with 5 µg/ml of mecillinam in bottom plates.

c, Growth of strain RM445 (*ΔftsZ/Δlpp/ΔlpoB*$_{sup}$) carrying the plasmid pOU82-ftsZ (with FtsZ, left panels) or none (No FtsZ, right panels), streaked on NA + 20mM Mg^{2+} in the absence (0) or presence (0.05) of 0.05 µg/ml of aztreonam.

Supplementary Tables

Supplementary Table 1: Genetic variation in *ftsZ*$_{sup}$ strains

	Base Position[a] (bp)	Genetic Variation	Gene name (synonym)	Type of Mutation	Gene function[b]
ΔftsZsup1	105305-106456	Deletion	*ftsZ*	Deletion of the gene *ftsZ* [6]	GTP-binding tubulin-like cell division protein
	1161341-1161903	Deletion of 562pb	*fhuE-hinT*	Deletion of the promoter region of the operon containing *lpoB*	*lpoB*: Outer membrane lipoprotein - activator of PBP1B activity
	2824993	A to G	*mltB*	Missense E195G	Membrane-bound lytic murein transglycosylase B
	3080013	T to G	*tktA*	Nonsense Y541Stop	Transketolase I
	3969949	T to G	*wzzE*	Missense Y307D	Enterobacterial Common Antigen polysaccharide chain length modulation protein
ΔftsZsup5	105305-106456	Deletion	*ftsZ*	Deletion of the gene *ftsZ* [6]	GTP-binding tubulin-like cell division protein
	165768	C to T	*mrcB*	Nonsense 347Stop	Penicillin-binding protein 1B (Pbp1B)
	1404427-1585557	Deletion of 181kb	*abgA-ydeP*	Multiple gene deletions	
	1757618-1757619	Deletion of a dinucleotides (CC)	*lpp*	Nonsense 74Stop	Murein lipoprotein (Braun's lipoprotein)
	2121458	Deletion of a nucleotide (C)	*wcaJ*	Nonsense 53Stop	Colanic acid biosynthsis UDP-glucose lipid carrier transferase
	2137438	G to A	*intergenic of wza-yegH*	n.a	
	3802322	T to A	*waaO (waaI)*	Missense N246I	UDP-D-glucose:(glucosyl)LPS α-1,3-glucosyltransferase
ΔftsZsup7	105305-106456	Deletion	*ftsZ*	Deletion of the gene *ftsZ* [6]	GTP-binding tubulin-like cell division protein
	1162915-1165932	Deletion of 3kb	*lpoB-intergenic of ycfP-ndh*	Multiple gene deletions containing lpoB	*lpoB*: Outer membrane lipoprotein - activator of PBP1B activity
	1391013-1589070	Deletion of 198kb	*ycjY-ydeT*	Multiple gene deletions (Rac prophage)	
	1750679-1761439	Deletion of 11kb	*ydhX-sufD*	Deletion containing the gene *lpp*	*lpp*: Murein lipoprotein (Braun's lipoprotein)
	2137438	G to A	*intergenic of wza-yegH*	n.a	
	2202729	T to C	*yehI*	Silent	Conserved hypothetical protein
	3802322	T to A	*waaO (waaI)*	Missense N246I	UDP-D-glucose:(glucosyl)LPS α-1,3-glucosyltransferase
	3969793	G to T	*wzzE*	Nonsense 255Stop	Enterobacterial Common Antigen polysaccharide chain length modulation protein

[a]Coordinate is based on NCBI RefSeq NC_000913.3 *E. coli* MG1655 Genome; [b]Gene function is based on EcoCyc Database; Red and Green colors represent genes respectively involved in peptidoglycan and extracellular polysaccharides synthesis

274

275 **Supplementary Table 2: Genetic variation in the *ΔftsZ/Δlpp/ΔlpoB*$_{sup}$ strain**

	Base Position[a] (bp)	Genetic Variation	Gene name (synonym)	Type of Mutation	Gene function[b]
ΔftsZ/Δlpp/ΔlpoB$_{sup}$	458026	G to A	*clpX*	Missense D201N	ATP-dependent serine protease
	105305-106456	Deletion	*ftsZ*	Deletion of the gene *ftsZ* [6]	GTP-binding tubulin-like cell division protein
	1162638-1163279	Deletion	*lpoB*	Deletion of the gene *lpoB* [7]	Outer membrane lipoprotein - activator of PBP1B activity
	1405207-1589365	Deletion of 184kb	*abgR-ydeT*	Multiple gene deletions	
	1757421-1757657	Deletion	*lpp*	Deletion of the gene *lpp* [7]	Murein lipoprotein (Braun's lipoprotein)
	2120046-2120848	Deletion of 802pb	*wzxC-wcaJ*	Troncation of wzxC and wcaJ genes	*wcaJ:* Colanic acid biosynthsis UDP-glucose lipid carrier transferase *wzxC:* Colanic acid exporter
	3811225	C to A	*intergenic of mutM-rpmG*	n.a	
	3969241	G to T	*wzzE*	Nonsense G71Stop	Enterobacterial Common Antigen polysaccharide chain length modulation protein
	4022740	C to A	*tatC*	Missense S2Y	TAT translocation system subunit

[a]Coordinate is based on NCBI RefSeq NC_000913.3 *E. coli* MG1655 Genome; [b]Gene function is based on EcoCyc Database; Green color represents genes involved in extracellular polysaccharides synthesis

276

277

Supplementary Table 3: Bacterial strains and plasmids used in this study

TB28	MG1655 *ΔlacIZYA*	5
RM349	TB28 *ΔftsZ::kan* pOU82-*Amp-ftsZ*	6
RM361	TB28 *ΔftsZ::kan sup1*	This study
RM362	TB28 *ΔftsZ::kan sup5*	This study
RM363	TB28 *ΔftsZ::kan sup7*	This study
RM380	TB28 *ΔlpoB::kan*	7
RM381	TB28 *Δlpp::kan*	7
RM382	TB28 *ΔmrcB::kan*	7
RM383	TB28 *ΔmrcA::kan*	7
RM384	TB28 *ΔlpoA::kan*	7
RM411	TB28 *ΔftsZ ΔlpoB::kan pOU82-Amp-ftsZ*	This study
RM413	TB28 *ΔftsZ Δlpp::kan pOU82-Amp-ftsZ*	This study
RM419	TB28 *ΔftsZ Δlpp ΔlpoB::kan pOU82-Amp-ftsZ*	This study
RM445	TB28 *ΔftsZ Δlpp ΔlpoB::kan sup**	This study
RM446	TB28 *ΔftsZ::kan sup5 pOU82-Amp-ftsZ*	This study
RM447	TB28 *ΔftsZ Δlpp ΔlpoB::kan sup* pOU82-Amp-ftsZ*	This study
RM448	TB28 *ΔftsZ Δlpp ΔmrcB::kan pOU82-Amp-ftsZ*	This study
RM449	TB28 *ΔftsZ Δlpp ΔmrcA::kan pOU82-Amp-ftsZ*	This study
RM450	TB28 *ΔftsZ Δlpp ΔlpoA::kan pOU82-Amp-ftsZ*	This study
RM451	TB28 *ΔftsZ ΔmrcB::kan pOU82-Amp-ftsZ*	This study
RM452	TB28 *ΔftsZ ΔmrcA::kan pOU82-Amp-ftsZ*	This study
RM453	TB28 *ΔftsZ ΔlpoA::kan pOU82-Amp-ftsZ*	This study

Plasmid	Relevant Genotype	Reference/Origin
pOU82-Amp-*ftsZ*	R1-replicon, *Amp lacZYA ftsZ*	6
pOU82-Cm-*ftsZ*	R1-replicon, C*m lacZYA ftsZ*	This study
pBAD33	pACYC184, *Cm araC Para*	Lab Collection
pBAD33-*lpoB*	pACYC184, *Cm araC* P_{ara}*-lpoB*	8
pBAD33-*lpp*	pACYC184, *Cm araC* P_{ara}*-lpp*	This study
pBAD33-*wcaJ*	pACYC184, *Cm araC Para-wcaJ*	This study
pBAD33-*mrcB*	pACYC184, *Cm araC Para-mrcB*	This study
pBAD24-*lpp*	pBR322, Amp *araC Para-lpp*	This study
pBS58	pGB2, *Sp ftsQAZ*	9
pKG339	pSC101, P_{lac}::*copA* Tet^R	10
pKD46-Sp	Sp^R, λ Red recombinase expression	6

kan, kanamycin; cat, chloramphenicol; tet,tetracyclin; Amp, b-lactamase; Sp,spectinomycin lacZ, b-galactosidase; P_{ara}, promoter arabinose; P_{lac}, promoter lactose

Supplementary Videos

Supplementary video 1: Time-lapse series showing *ΔftsZsup5* cells growing on NA. Phase contrast images were acquired automatically every minute for about 87 min. Scale bar is 3 µm.

Supplementary video 2: Time-lapse series showing *ΔftsZsup1* cell growing on NA 20mM Mg^{2+}, from which the panels in Figure 2b were obtained. Phase contrast images were acquired automatically every minute for about 279 min. Scale bar is 3 µm.

Supplementary video 3: Time-lapse series showing *ΔftsZsup7* cell growing on NA 20mM Mg^{2+}. Phase contrast images were acquired automatically every minute for about 109 min. Scale bar is 3 µm.

Supplementary video 4: Time-lapse series showing *ΔftsZsup7* cell dividing on NA 20mM Mg^{2+}, from which the panels in Figure 2b were obtained. Phase contrast images were acquired automatically every minute for about 69 min. Scale bar is 3 µm.

Supplementary video 5: Time-lapse series showing *ΔftsZsup* cell dividing on NA + 20 mM Mg^{2+}, from which the panels in Figure 2c were obtained. Phase contrast images were acquired automatically every minute for about 90 min. Scale bar is 3 µm.

Supplementary video 6: Time-lapse series showing RM445 (*ΔftsZ/Δlpp/ΔlpoB*$_{sup}$) cell, bearing the plasmid pBAD33-*lpoB* cell growing on NA + 20 mM Mg^{2+} with glucose (lpp expression repressed). Phase contrast images were acquired automatically every minute for about 209 min. Scale bar is 3 µm.

Supplementary video 7: Time-lapse series showing RM445 (*ΔftsZ/Δlpp/ΔlpoB*$_{sup}$), bearing the plasmid pBAD33-*lpoB* cell growing on NA + 20 mM Mg^{2+} with *lpoB* expression induced (arabinose), from which the panels in Figure 3d were obtained. Phase contrast images were acquired automatically every minute for about 209 min. Scale bar is 3 µm.

Supplementary References

1 Sledjeski, D. D. & Gottesman, S. Osmotic shock induction of capsule synthesis in *Escherichia coli* K-12. *J Bacteriol* **178**, 1204-1206, (1996).

2 Glover, W. A., Yang, Y. & Zhang, Y. Insights into the molecular basis of L-form formation and survival in *Escherichia coli*. *PloS One* **4**, e7316, (2009).

3 Bendezu, F. O. & de Boer, P. A. Conditional lethality, division defects, membrane involution, and endocytosis in *mre* and *mrd* shape mutants of *Escherichia coli*. *J Bacteriol* **190**, 1792-1811, (2008).

4 Donachie, W. D. The cell cycle of *Escherichia coli*. *Annu Rev Microbiol* **47**, 199-230, (1993).

5 Bernhardt, T. G. & de Boer, P. A. The *Escherichia coli* amidase AmiC is a periplasmic septal ring component exported via the twin-arginine transport pathway. *Mol Microbiol* **48**, 1171-1182, (2003).

6 Mercier, R., Kawai, Y. & Errington, J. General principles for the formation and proliferation of a wall-free (L-form) state in bacteria. *Elife* **3**, (2014).

7 Baba, T. *et al.* Construction of *Escherichia coli* K-12 in-frame, single-gene knockout mutants: the Keio collection. *Molecular Systems Biology* **2**, 2006 0008, (2006).

8 Typas, A. *et al.* Regulation of peptidoglycan synthesis by outer-membrane proteins. *Cell* **143**, 1097-1109, (2010).

9 Bi, E. & Lutkenhaus, J. FtsZ regulates frequency of cell division in *Escherichia coli*. *J Bacteriol* **172**, 2765-2768, (1990).

10 Jensen, R. B., Grohmann, E., Schwab, H., Diaz-Orejas, R. & Gerdes, K. Comparison of *ccd* of F, *parDE* of RP4, and *parD* of R1 using a novel conditional replication control system of plasmid R1. *Mol Microbiol* **17**, 211-220, (1995).